We are IntechOpen, the world's leading publisher of Open Access books Built by scientists, for scientists

4,800
Open access books available

122,000
International authors and editors

135M
Downloads

Our authors are among the

154
Countries delivered to

TOP 1%
most cited scientists

12.2%
Contributors from top 500 universities

CLARIVATE ANALYTICS BOOK CITATION INDEX INDEXED

WEB OF SCIENCE™

Selection of our books indexed in the Book Citation Index in Web of Science™ Core Collection (BKCI)

Interested in publishing with us?
Contact book.department@intechopen.com

Numbers displayed above are based on latest data collected.
For more information visit www.intechopen.com

15

An Active Technology for Improving the Sound Transmission Loss of Glazed Facades

Berardo Naticchia, Alessandro Carbonari and Sara Spadoni
Polytechnic University of Marche
Department of Architecture Construction and Structures
Italy

1. Introduction

The 89/106/CEE European Directive and the related national legislation of the European member countries have made noise protection a compulsory building requirement. From an acoustic point of view, building envelopes have the task of reducing external noise to an acceptable level inside the same building.
In fact, glazed facades are the preferred paths followed by disturbing noise from the outside to the inside and, in spite of the adoption of very expensive passive means, they are often unable to respect the strict limits required by standards and regulations. The two main types of passive means used are: laminated glass technology or double glazing. Both of these can be useful for reducing noise transmission at high frequencies: in particular the laminated solution is used to shift the coincidence effect at frequencies higher than the audible range, in fact improving STL values in the range of acoustic waves higher than 1500 Hz, while determining no improvements at lower frequencies. On the other hand, in double glazing, the coupling between the glass panels and the air layer adds another resonance effect at frequencies lower than 500 Hz, while improving their STL in the range of frequencies limited between the resonance and coincidence effects. As a consequence, the adoption of an active control system is needed to solve the acoustic performances drop of glass panels at low frequencies.
This chapter will show how an active system would be capable of controlling the vibrations of glazed panels and of reducing sound radiated as a consequence, avoiding the use of very expensive glazed facades equipped with massive passive means and effective only at high frequencies, whose adoption would also raise economic and technologic problems for their installation on buildings. In particular, the ASAC (Active Structural Acoustic Control) approach will be analyzed and tested, also demonstrating why it is better than the other Active Noise Control approach, commonly known as ANC. Pursuing this aim requires tackling a series of complex problems such as choosing reference and error sensors, modelling the system controller, designing the system with well-suited actuators, integrating the active system into typical glazed façades while minimizing visual impact and maximizing the controllability of structural vibrations. It will be shown that remarkable sound transmission loss (STL) improvements can be obtained and that this approach has great exploitability potential in other specialized products like light opaque building partition walls, railway and traffic noise shielding, temporary environmental noise barriers or even real-time controlled reflecting panels for the acoustic adjustment of concert halls.

2. State of the art and the innovation provided by ASAC systems for glass panels

2.1 Early Active Noise Control applications

The concept of active noise control was first introduced by Leug (Leug, 1936), who presented a patent for a system implementing feed-forward active control of sound in a duct. According to the patent, the sound field is detected using a microphone, whose signal is passed through an electronic controller, such that it adjusts the loudspeaker to produce a cancelling wave in a duct, resulting in destructive interference of the primary or noise source wave. A feed-back arrangement was produced by Olson and May (Olson et al., 1953), who developed an active noise control system that is based upon detecting the offending sound with a microphone and feeding the signal back through a controller to a control loudspeaker located close to the microphone. They also demonstrated good local reduction at the microphone over a range of frequencies from 20 to 300 Hz.

Conover (Conover, 1955) introduced the concept of an error sensor in which the radiated sound field of the transformer was monitored and used to adjust the controller in order to minimize the radiated sound. However, he experienced difficulties due to the use of analogue systems, particularly when the physical system was changing relatively rapidly.

Hence, in the early 1970s both (Kido, 1975) and (Chaplin et al., 1976) began exploring the application of digital signal processing techniques, demonstrating the feasible use of their digital active noise control approaches on a number of important applications, such as car exhaust noise, ship exhaust stack noise and active engine mounts.

2.2 Active control of structural vibrations

The introduction of digital techniques and piezoelectric actuators to vibration control by Bailey & Hubbard (1985) considered feedback modal control of large structures. Balas & Canavin (1977) discussed feedback damping control of large spacecraft structures. Balas (1978) applied theoretical modal control using velocity feedback to a simple beam. Meirovitch & Öz (1980), with later work by Meirovitch and others (e.g. Meirovitch et al., 1983), expanded the modal control method, finally arriving at a method they described as Independent Modal-Space Control (IMSC), where a coordinate transformation was used to decouple a complicated system into a set of independent second order systems in terms of modal coordinates.

Baz & Poh (1988) made modifications to the IMSC method to minimize the effect of control spillover (inadvertent localized increases in vibration levels due to constructive interference between disturbance and control fields). Modern applications include precision optical components in noisy environments, pilot seat vibrations in helicopters, sonar masking in torpedoes and submarines.

2.3 Active Structural Acoustic Control

Advances in active control of structural vibrations have been applied to develop an alternative control method for enclosed noise fields, known as active structural acoustic control (ASAC). The ASAC approach uses structurally-based actuators to exert control forces on the radiating structure itself in order to minimize radiated sound (Ruckman & Fuller, 1995; Nelson & Elliott, 1995; Fuller et al., 1996). The actuators are vibration sources (shakers, piezoceramic patches, etc.) which modify how a structure vibrates, thereby altering the way it radiates noise.

In 1990 Jones and Fuller proposed an initial work where electromagnetic shakers were used to provide point force control inputs to simplified cylindrical test sections. The controller exploited error sensor microphones placed in the cylinder interior, such that interior sound levels were minimized by the control of structural vibration. This work demonstrated that, in general, fewer control actuators are required by the ASAC approach as compared to ANC (Active Noise Control) techniques. Also, control spillover in the interior acoustic space was reduced in the ASAC experiments. In such cases, "modal suppression" is usually suggested, where only the few dominant radiating modes are reduced in amplitude. Other structural modes that are poorly coupled with the noise field may be left unchanged by the control system (Fuller et al., 1996).
Simpson, et al. (1991) performed control experiments in a test section comprising the aft portion of a furnished DC-9 aircraft. Using a typical feed-forward controller arrangement, the researchers achieved global sound level reductions of up to 9 dB using various configurations of 7 error microphones.
Because point forces are spectrally white in a spatial sense, their use as controlling forces in ASAC work can lead to undesired spillover in many structural vibration modes. In seeking a control actuator with more distributed forcing properties, many researchers recently investigated the use of piezoceramic materials for applying bending moments or in-plane strains to structures (Clark et al., 1991). In particular, lead zirconium titanate (PZT) materials have been widely used in ASAC work, providing sufficient forcing capabilities with the benefit of greatly reduced mass and space requirements as compared to electromagnetic shaker devices.
In 1992 Fuller et al. used an aluminium cylindrical test section with a removable floor structure to simulate an aircraft fuselage environment. Piezoelectric patches were bonded directly to the cylinder surface and the system was acoustically excited with an exterior loudspeaker noise source. Using two microphones as error sensors, the ASAC system provided global attenuations on the order of 10 dB in the cylinder interior.
Recently, ASAC tests were performed by Fuller et al. (1994) in the cabin of a Cessna fuselage, a typical mid-sized business jet. In the acoustic resonance case, noise reductions of 20 dB or more were achieved at the error sensors, but an average global increase of several dB was measured at 7 additional microphones. Control performance in the off-resonance case was significantly reduced, with reductions of 2-10 dB at the error sensors.
Some past work has addressed actuator position optimization via analytical approaches (Clark et al., 1992; Wang et al., 1994; Burdisso et al., 1994). Additionally, one work with a finite element model has shown the importance of position optimization to global ASAC performance, made by (Yang et al., 1995). Spatially averaged reductions of acoustic potential energy of up to 14 dB have been predicted using 16 optimally-located point forces, while poor control force placement may result in overall global sound increases.

2.4 Active Noise Control in glazed enclosures

To the authors' knowledge, no ASAC application has been performed on glazed structures. Other works by (Kaiser et al., 2003) suggest an ANC approach through the positioning of both loudspeakers and sensors inside air cavities; and (Zhu et al., 2004) place monitoring sensors outside windows. Instead, most of the recent research was developed to verify the performances of the control provided by PZT patch actuators on opaque surfaces, both for building walls and for helicopter and airplane envelopes: in the contributions of (Kaiser et

al., 2003) and (Bao and Pan, 1997) it is shown that using ANC control systems for double walls needs cavities wider than 0.1 m thick, which is not usual for standard double glazed panels. Preliminary results in Wernli (2001) show that PZT laminated (multi-layer) patches can indeed actuate the heavy panes sufficiently. However, since these patches interfere substantially with the primal function of the window, namely to look through it, they may not be considered an option.

2.5 The original contribution provided by the proposed ASAC system for glass panels

The research described in this chapter proposes an original approach for applying ASAC on glazed structures, which takes into account the problem of using piezo stack actuators, whose visual impact must be managed, even if considerably reduced compared to the piezo-laminated patch actuators.

The application of ASAC systems on glazed panels is particularly critical, as there are no means of efficiently increasing their STL over all the acoustic spectrum, as will be explained in paragraph 3.1. For example, acoustic interlayers provide the most significant noise reduction in the frequency range of 1500 to 6000 Hz, while in the range of 100 to 500 Hz the Sound Transmission Loss remains significantly low. Furthermore, the double glazing approach provides appreciable noise reduction just in the frequency range above 500 Hz.

Hence the use of the ASAC technology seems to be the only one capable of increasing glazed facades' STL over all the acoustic spectrum. In this way, it would be possible to respect the strict European and national legislation on expected acoustic performance for external facades, even in very harsh areas, such as in proximity of airports, railways or high traffic roads. Additionally, the problems connected with the application of actuators on transparent facades will be tackled for the first time.

3. Adoption of active means for controlling acoustic and vibration behaviour of glass panels

3.1 Adoption of active means for STL increase

Considering that for buildings, the main type of disturbing noise is produced by road and railway traffic, panels excited by plane waves have been studied. Analytical solutions for forecasting the behaviour of unbounded non flexible panels are known (Fahy, 1985), and they can be easily extended to building envelopes. The STL of glass alone at low frequencies is determined by the panel's static stiffness. Since glass reacts best to excitation frequencies that match its natural frequencies, the low internal damping of tempered glass produces resonances that dramatically decrease its STL. Above the resonant frequencies, sound transmission follows the mass law of acoustics and is dictated by the mass or surface density of glass. However, glass has a specific coincidence frequency at which the speed of incident acoustical waves matches that of the glass bending wave and acoustic waves are especially effective at causing glass to vibrate, which makes the vibrating glass an effective sound radiator at that specific frequency and above. As a result, the first critical point for a single glass panel is in correspondence of the resonance effect (f_R), registered at very low acoustic frequencies, as in Fig. 1-a (Spagnolo, 2001). Above this value its STL increases with frequency, until the critical effect causes another drop of STL, due to the matching between the wavelength of flexural vibrations propagating through the glass and the projection of the disturbing noise wavelength which dramatically increases the overall radiation efficiency of the glass panel. The latter effect may be solved through the adoption of

laminated glass panels with PVB layers, which decrease the overall flexural stiffness of laminated panels, shifting up the critical frequency (f_C), out of the audible range. But no remarkable improvements are obtained at the resonance frequency. Even if double glazing provides an average increment of STL (moreover in the middle frequency range), however it generates another resonance frequency, due to the coupling between the two glass panels and the air cavity, whose position depends on the thickness and typology of the panels (Harris, 1984). An illustrative example from measurements is presented in Fig. 1-b, based on (Harris, 1994): three double glass panels are compared in order to point out the importance of the air layer thickness with respect to the final STL. Starting from a good double glazing (two 0.006 m thick glass panels with a 0.013 m air layer interposed) it is demonstrated that even if the air layer is further widened, the low frequency STL is still low due to resonance dip which persists even if a much higher air thickness equal to 0.05 m is provided.

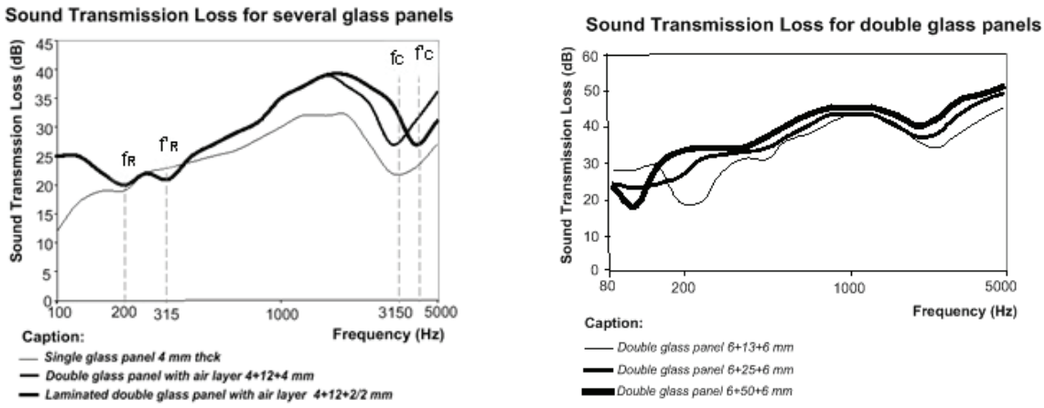

a) b)

Fig. 1. Sound Transmission Loss curves for single, double and laminated glass panels (a); the same for double glass panels (b).

Moreover, considering that traffic noise levels are usually very high in the low frequency range (IMAGINE, 2003), it follows that other solutions are required for guaranteeing acoustic comfort in buildings (as illustrated in Fig. 2).

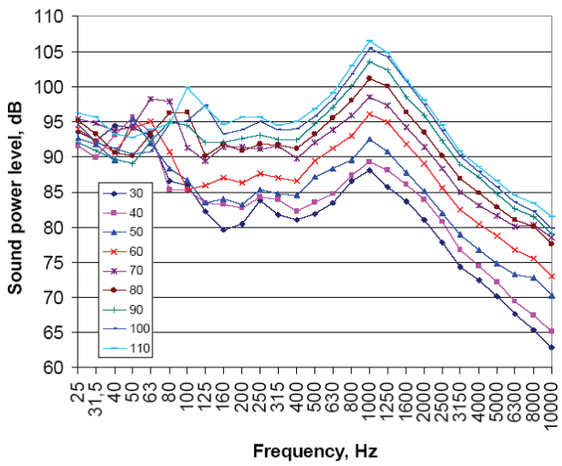

Fig. 2. Equivalent omni-directional sound power level of road traffic noise as function of a vehicle's speed.

3.2 Analytic model for the simulation of vibrating glass panels

As flexural waves in structures are the main responsible agents for sound emission (Hall, 1987) and they are induced in plates by external disturbances, it is opportune to analytically describe the flexural response of a simply supported plate to a harmonic excitation of arbitrary distribution like $f(x,y,t) = F(x,y) \cdot e^{i\omega t}$ (where $\omega = 2\pi\nu$, ν is the excitation frequency, $F(x,y)$ is the excitation amplitude), obtaining the equilibrium model introduced by Kirchhoff-Love (Timoshenko and Woinolowsky-Krieger, 1959):

$$EI\left(\frac{\partial^4 w}{\partial x^4} + 2\frac{\partial^4 w}{\partial x^2 \partial y^2} + \frac{\partial^4 w}{\partial y^4}\right) + \rho h \frac{\partial^2 w}{\partial t^2} = -F(x,y)e^{i\omega t} \tag{1}$$

being i the complex unit, w the transversal displacement, E, I, ρ and h the elasticity modulus, moment of inertia, density and thickness, respectively, of the plate. One of the possible solutions of eq. (1) for the formalization of the transverse displacement field is obtained describing it as the superposition of infinite modes of the free response of the plate, which is vibrating at the forcing frequency:

$$w(x,y) = \sum_{m=0}^{\infty}\sum_{n=0}^{\infty} W_{m,n}\Psi_{m,n}(x,y)e^{i\omega t} \tag{2}$$

where $W_{m,n}$ are the modal amplitudes, which are the maximum displacements at the free natural mode *(m, n)*. $\Psi_{m,n}$ are the modal shapes, which take into account the shape of the mode *(m,n)* on the plate, while the exponential term is aimed at describing the dependence with the time and the influence of disturbing frequency. In order to study the transversal displacement motion of a plate whose side lengths are a and b, it is necessary to compute the displacement distribution field given by an incident plane wave. Eq. (2) is generally approximated in another form, which considers only the superposition of a finite number of vibrating modes, given by the combination of two finite numbers m and n (the validity of the approximation is dependent on the choice of these two values). Thus the displacement distribution is given by (Fuller et al., 1997):

$$w(x,y,t) = \sum_{m=1}^{M}\sum_{n=1}^{N} W_{m,n}\,\mathrm{sen}(k_m x)\cdot\mathrm{sen}(k_n y)e^{i\omega t} \tag{3}$$

where the eigenvalues are:

$$k_m = \frac{m\pi}{a},\ k_n = \frac{n\pi}{b} \tag{4}$$

Substituting eq. (3) in eq. (1) we can find the solution as:

$$W_{m,n} = \frac{P_{m,n}}{\rho h\left(\omega_{m,n}^2 - \omega^2\right)} \tag{5}$$

being $P_{m,n}$ the modal pressure, that is, the action given separately by each mode of vibration, $\omega_{m,n}$ the natural frequencies of the glass plate as reported in (Fahy, 1985):

$$\omega_{mn} = \sqrt{\frac{EI}{\rho h}\left[\left(\frac{m\pi}{a}\right)^2 + \left(\frac{n\pi}{b}\right)^2\right]} \tag{6}$$

In (Roussos, 1985) an analytical solution for the generic case of a plane wave incident on a simply supported plate, like in Fig. 3, is detailed.

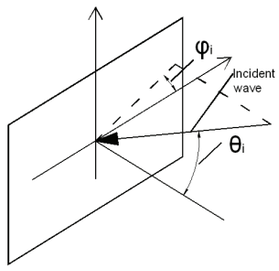

Fig. 3. Angles individuating the direction of incidence of an acoustic plane wave into a glazed plate.

4. The ASAC active control system adopted

4.1 Active Structural Acoustic Control

The approaches by Leug's patent in 1936 and (Olson & May, 1953) are the first examples of ANC feed-forward control, when prior knowledge of the noise is obtained with an upstream microphone, and ANC feedback arrangement, where the detection microphone is close to the active secondary source respectively. Both approaches relate to the main concept of ANC, and hold its drawbacks: when applied to buildings' glazed facades, they need an external microphone for disturbance monitoring, and internal error sensors and loudspeakers for control purposes. For this reason some attempts at inserting all the system components inside the air cavity of double walls were pursued but this task became much too difficult in the case of windows, due to their narrow air layers.

Therefore, the ASAC system should be preferred for this kind of application, because both reference sensors and actuators are placed on the same glazed panel, as required for the implementation of a feedback controller. Fig. 4-a and Fig. 4-b respectively depict the feed-forward and feed-back arrangements of an ASAC configuration for glazed facades' control. In both cases, actuators are positioned on the vibrating surface, which is the source of disturbing noise in the receiving room and whose vibrations are reduced to rise its final STL. ASAC does not require the use of loudspeakers or error microphones in the receiving environment, however optimum positioning of sensors and PZT actuators on the vibrating surface must be pursued. Generally, various modes of vibration have different radiation efficiencies (Fahy, 1985), and some are better coupled to the radiation field than others. This suggests two conclusions: only the most efficient modes need to be controlled, rather than the whole response; in some cases the relative phases and amplitudes of multi-modal response can be adjusted so that their radiated fields interfere destructively.

The feed-forward control of Fig. 4-a requires knowledge of the primary disturbance, which is derived by the use of a reference microphone: in the case of buildings, this seems unpractical, because it would require the installation of a microphone on the exterior of the

window which, for functional and aesthetic issues, is not feasible. Therefore, the feedback type controller depicted in Fig. 4-b seems to be opportune and is detailed subsequently.

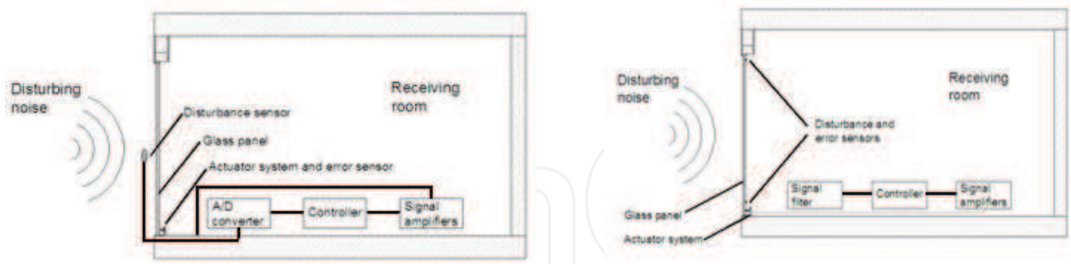

Fig. 4. Feed-forward (case a) and feedback (case b) ASAC systems for glazed facades.

4.2 Optimal control theory

The ASAC approach is based on the reduction of structural vibrations and radiated sound (transmitted and reflected) as a consequence, by means of actuators bonded on the vibrating surfaces. ASAC can be easily integrated into buildings, as it does not require the use of loudspeakers or error microphones in the receiving environment.

As shown in Fig. 5, once the signal comes from the sensors, it must be elaborated by charge amplifiers (converting voltage signals into physical variables like displacements, velocity and accelerations), and electronic filters that have a double task:

- to separate the contribution to the total vibration field due to the primary disturbance from that due to secondary sources;
- to compute the radiated field in some positions of the receiving room, to calculate the error (difference between reference value and actual value of the radiated noise).

The controller, starting from the error signals, computes the opportune voltage to be supplied to the secondary sources, whose electric power is provided by the amplifiers. At this level an algorithm calculates the control voltage to be supplied to the secondary sources. In general, it has the task of changing the distributed mass, stiffness and damping of the plate in order to reduce the radiated noise in the internal environment, determined mainly by flexural waves which need to be decreased by the control plant for this reason. The complexity of the algorithm derives from the fact that reference and control sensors are positioned at the same place, therefore electronic filters are necessary. The controller must opportunely tune its gain coefficients to adjust the properties of the system, so that the radiated noise will be minimized. A number of papers, such as (Baumann et al., 1992), (Cunnefare, 1991), (Baumann et al., 1991) and (Pan et al., 1992), showed that optimum control is the most suitable for ASAC systems: it has the advantage that the choice in the prescribed change of the dynamic properties is motivated by its aim to reduce structural vibrations or radiated noise.

Optimal control system procedures offer the possibility of designing the controller parameters directly minimizing a cost function of performance which is proportional to the required measure of the system's response. For the sake of computational efficiency, it is convenient to define a cost function that is quadratically dependent on the response, simplifying the optimization problem. One of the possible solutions can be the one proposed by (Fuller et al., 1997), where the cost function is given by:

$$J = \frac{1}{2\rho c} \sum_{i=1}^{N} \left| p_t^i \right|^2 \Delta S_i \tag{7}$$

being J the total radiated acoustic power, ρ and c the density and sound velocity of wave in air; p_i the sound pressure values measured at some prescribed measurements points and ΔS_i the surfaces relative to each measurement point. Pressure values are not directly measured, but computed from the signals deriving from the reference sensors positioned on the glazed panel (through the use of filters). Thus, the structural-acoustic coupling is inherent in the definition of the cost function. It was demonstrated by (Fuller et al.,1997) and (Nelson & Elliott, 1992) that substituting the opportune expression of radiated sound pressure, given

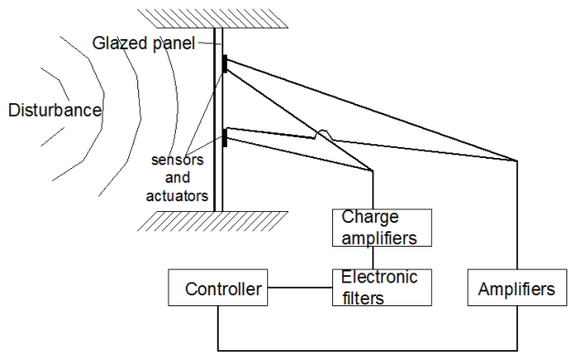

Fig. 5. Scheme of an ASAC system for glazed panels integrated in buildings

by the superposition of the two contributions of both the disturbance and the control actuators, the cost function is scalar. It can be converted into a quadratic expression of complex control voltages, and it was demonstrated that this function has a unique minimum. The general form of the equation to be minimized becomes:

$$J = \underline{h}^T \underline{q} + \underline{c}^T \underline{v}_i \tag{8}$$

where q is the vector of complex input disturbances, h is the vector of transfer functions associated with these disturbances; c is the control transfer function vector and v is the unknown vector. In this way a vector of voltages v_i is computed, minimizing the total radiated field.

Once the transfer functions between the reference signal deriving from reference sensors and the acoustic radiated noise is known for a given system, the control plant will automatically execute all these steps, minimizing the radiated noise even if glazed panels are subject to time-dependent input disturbances, giving back an automated glazed facade, that actively changes its properties according to the disturbance. Before implementing this control system, it is necessary to calculate the control transfer functions, which requires as a preliminary stage, the choice of the opportune kind of secondary sources, carried out in the next section.

However, the analytical model can be implemented only following a series of simplifications, which appear difficult to apply in terms of the actual situations that one can come across in the building field:

- simple support boundary constraints, whereas in fact, constraint situations are more complex and more similar to a semi- fixed or yielding joint;
- applications of only point forces, without the association of mass as occurs in the real case when control is effected through the use of actuators contrasted by stiffening structures.

Given the above considerations, it has been established that the numeric model based on the theory of Kirchhoff-Love, will be substituted by a model built using finite element software programs (ANSYS™, LMS VIRTUAL LAB™), which allows overcoming the simplifications tied to the analytic model.

4.3 Piezoelectric actuators

Two main types of actuators, suitable for glazed facades, are presently marketed (Fig. 6):

- Piezoelectric (PZT) patch actuators providing bending actions to excite structures;
- PZT stack actuators providing point forces to excite structures.

a) b)

Fig. 6. PZT patch (a) and stack actuators for glazed facades (b).

The first type is usually bonded to a surface while the second needs a stiffening structure to fix it and make it transfer forces to a surface for controlling purposes. These actuators are available in a wide range of sizes (from few centimetres to various decimetres) and are capable of generating high forces (with reduced displacements) inside a wide range of frequencies (Dimitriadis, Fuller, Rogers, 1991). Even if they were shown to work properly for many applications, however they have not been tested in applications on glazed facades, and most of the experiments were carried out in the automotive and aeronautic fields of research. As far as concerns the choice of actuators, the first rectangular shaped patch may interfere with visibility (Fig. 7-a); the stack one instead is very small but needs a stiffener in order to work properly (Fig. 7-b).

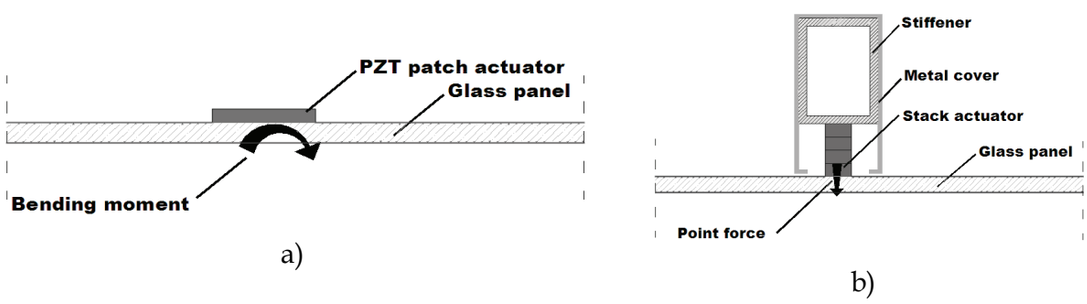

a) b)

Fig. 7. PZT patches (a) and PZT stack actuators (b), as applied on a glass panel.

In the asymmetric disposal of Fig. 7-a, the PZT patch excites the 2D structure with pure bending, that can be simulated with the numerical model developed in (Dimitriadis, Fuller, Rogers, 1991). It is assumed that the strain slope is continuous through the thickness of the glass plate and of the PZT patch, but different along the directions parallel to the plate sides, which in turn are assumed parallel to the coordinate axes (the strain slopes are billed C_x and C_y). The mathematical relation between strain and z-coordinate is:

$$\varepsilon_x = C_x \cdot z \text{ and } \varepsilon_y = C_y \cdot z \tag{9}$$

being the origin of the z-axis in the middle of the plate thickness and ε the strain. The unconstrained strain of the actuator (ε_{pe}) along plate axes is dependent to the voltage applied (V), the actuator thickness (h_a) and the PZT strain constant along x or y directions ($d_x = d_y$):

$$\varepsilon_{pe} = \frac{d_x V}{h_a} \tag{10}$$

Considering that the plate is subject to pure bending, no longitudinal waves will be excited, and by applying the moment equilibrium condition about the centre of the plate along x and y directions as in (Fuller, Elliott, Nelson, 1997), assuming that the plate thickness is $2h_b$, the plate elastic modulus is E_p, the actuator elastic modulus is E_{pe}, and ν_p and ν_{pe} are the Poisson coefficients of the plate and actuators respectively; also assuming that moments induced in the x and y directions (billed with m_x and m_y) are present only under the PZT patch, and assuming that it is located between the points of coordinates (x_1,y_1) and (x_2,y_2), in (Dimitriadis, Fuller, Rogers, 1991) it is shown that:

$$m_x = m_y = C\varepsilon_{pe}\left[H(x-x_1)-H(x-x_2)\right]\left[H(y-y_1)-H(y-y_2)\right] \tag{11}$$

being $H(x)$ the Heaviside function and $C=EIK_f$, where I is the moment of inertia of the plate; then the equation of motion for plates subject to flexural waves can be written:

$$EI\left(\frac{\partial^4 w}{\partial x^4}+\frac{\partial^4 w}{\partial y^4}\right)+\rho h\frac{\partial^2 w}{\partial t^2}=-p(x,y) \tag{12}$$

where p is an external uniform pressure applied on the plate. Eq. (11), if written with the actuator induced moment, becomes:

$$\frac{\partial^2\left[M_x(x)-m_x(x)\right]}{\partial x^2}+\frac{\partial^2\left[M_y(y)-m_y(y)\right]}{\partial y^2}-\omega^2\rho S w=0 \tag{13}$$

where M is the internal plate moment and m is the actuator induced bending moment; ρ and S are density and surface of the plate; w is the displacement and ω is the wave phase change. Assuming that the actuator is perfectly bonded on the glass plate and substituting (11) inside (13), the solution of (12) can be calculated by using the modal expansion of (3), which gives back:

$$W_{mn} = \frac{4C_0\varepsilon_{pe}}{\rho h mn\,\pi^2\left(\omega_{mn}^2-\omega^2\right)}\left(k_m^2+k_n^2\right)p_1 p_2 \tag{14}$$

where: $p_1 = cos(kmx_1) - cos(kmx_2)$, $p_2 = cos(kny_1) - cos(kny_2)$.

Equation (14) can be written in terms of (3) and (5), defining the variable:

$$P_{mn} = \frac{4 C_0 \varepsilon_{pe}}{mn \pi^2} \left(k_m^2 + k_n^2 \right) p_1 p_2 \tag{15}$$

Thus, given the properties of the PZT patches under use and the ones of the plate, (14) together with (5) and (3) gives back the transversal displacement function on the 2D plate caused by PZT patch actuators with respect to *x* and *y* coordinates. In the case shown in Fig. 7-b, the stack actuator has the task of providing a punctual force, instead of a bending moment. Following a procedure similar to the one explained above, it is possible to calculate a numerical model that describes the vibration field in terms of (3) and (5) exploiting the following relation:

$$P_{mn} = \frac{4 F_a}{ab} \sin k_m x_f \sin k_n y_f \tag{16}$$

where *a* and *b* are the side lengths of the plate; x_f and y_f are the coordinate of the point where the force F_a is applied, that is the action provided by the stack actuator, which is dependent to the reaction system stiffness. Assuming d_z the strain constant of the actuator along the z-direction, its unconstrained displacement will be computed by:

$$w_a = \frac{d_z V}{L_a} \tag{17}$$

where L_a is its height. In fact the real displacement of the stack is lower than (16) because the reaction system has finite stiffness *K*, and the force effectively exerted by the stack along the z-direction is:

$$F_a = \frac{d_z V K}{1 + \frac{K}{K_a}} \tag{18}$$

being *ka* the actuator stiffness. As in the previous case, the transverse vibration displacement of a 2D plate can be calculated by (14) with (5) and (3).

In the following numerical simulations, performed according to the model described above, the disturbance is assumed to be a wave with frequency near the frequency of the mode of vibration (2,2) of a typical building façade's panel, whose effect is compared with the one given by the use of the two aforementioned kinds of actuators. The glazed panel is supposed to be simply supported along the edges. The two configurations of Fig. 7 are studied analytically. The properties of the glazed plate used for these simulations are listed in Tab. 1, while for PZT patches in Tab. 2. For the simply supported plates of Tab. 1, natural frequencies of vibration are given by (6), whose results are listed in Tab. 3 for the smallest modes; so the frequency of the disturbance was chosen equal to 78 Hz. In the first case of Fig. 7-a, the behaviour of the panel of Tab. 1 is simulated when equipped with two dispositions of PZT patches:

- 8 patches equally distributed 0.05 *m* far from the panel edges;
- 26 patches equally distributed 0.05 *m* far from the panel edges.

Each rectangular shaped patch measures (0.05 x 0.04) *m*. Fig. 8 shows the distribution of the maximum amplitude vibration field along the middle axis of the plate, computed along the y=l/2. One of the diagrams is referred to the effect due to the disturbance wave at frequency v = 78 Hz and intensity 100 dB. For a voltage of 150 V (that is the highest limit for low-voltage actuators) PZT patches can generate vibration fields far lower than the one generated by the disturbance.

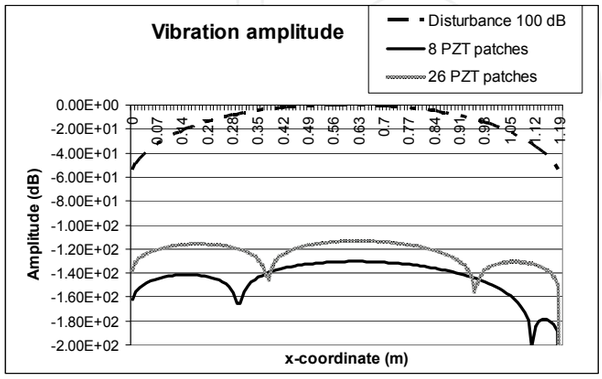

Fig. 8. Amplitude displacement along the y=l/2 axis due to the positioning of PZT patches actuators, normalized with respect to the maximum disturbance value.

In the second case vibration amplitudes are computed for the stack configuration shown in Fig. 7-b. In Fig. 9 such vibration amplitudes are drawn with dependence to the voltage provided to stack actuators. It is assumed that the panel is equipped with 3 actuators (0.02 *m* long with $7.8 \cdot 10^{-5}$ m^2 cross sectional area) per each side, equally spaced and at a 0.03 *m* distance from the two edges; the stiffness of the reaction system is assumed equal to 200 *N/μm*. Fig. 9 shows that, regardless of the small rigidity of the reaction system, the stack actuators can produce a vibration amplitude comparable with the one due to the disturbance with only a voltage of 100 V.

Symbol	QUANTITY	Units of measurement	Value
E_p	Modulus of elasticity	Pa	$6..9 \cdot 10^{10}$
ν_p	Poisson coefficient	-	0.23
ρ_p	density	Kg/m^3	2457
h_p	thickness	m	0.006
l_p	Side length	m	1.2

Tab. 1. Glazed plate's properties.

Symbol	QUANTITY	Units of measurem.	Value
E_{pe}	Modulus of elasticity	Pa	$6.3 \cdot 10^{10}$
ν_{pe}	Poisson coefficient		0.3
ρ_{pe}	density	Kg/m^3	7650
h_{pe}	thickness	m	0.0002
d_{31}	Expansion constant	m/V	-0.000000000166

Tab. 2. PZT patch's properties.

Mode	FREQUENCY (HZ)	Mode	Frequency (Hz)
(1,1)	20.6	(2,2)	82.4
(1,2)	51.5	(2,3)	133.8
(1,3)	102.9	(3,3)	185.2

Tab. 3. Natural frequencies of vibration.

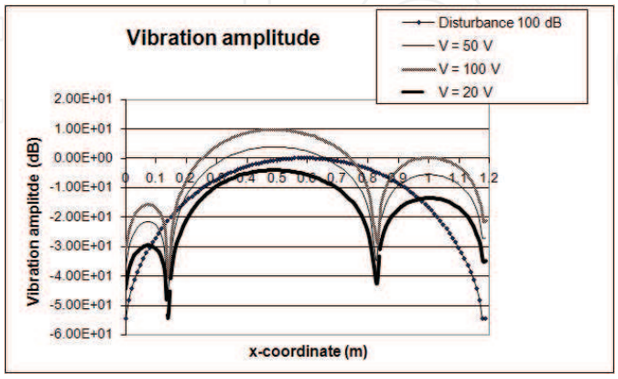

Fig. 9. Amplitude displacement along the y=l/2 axis due to the positioning of stack stiffened actuators, normalized with respect to the maximum disturbance value.

Therefore, given the high controllability provided by stack actuators, they have been considered suitable for controlling glazed facades and they have been object of the experimental campaign and technologic development carried out in this research.

5. The case study: An Active Structural Acoustic control for a window pane

5.1 The components of ASAC System for glazed facades

In paragraph 4.2 the two basic arrangements for an ASAC system configuration have been introduced, that are feed-forward and feed-back types. As already discussed, the first one requires the knowledge of the primary disturbance, which implies the use of a reference microphone. This solution seems to be unpractical for the suggested application, requiring the installation of a microphone on the exterior of the window, unfeasible for functional and aesthetical issues. Hence, the feedback arrangement is preferred by the authors and detailed in the following pages.

The components of a feedback ASAC system for glazed facades are (Fig. 10):

- sensors for detecting vibration (e.g. strain gauges);
- electronic filters for analyzing signals from sensors in order to check the vibration field induced by disturbance;
- an electronic controller for manipulating signals from the sensors and compute the most efficient control configuration at the actuators level;
- charge amplifiers for driving secondary actuators on glazed panels according to the outputs sent by the controller;
- actuators for controlling the vibration field of glazed panels.

As seen in paragraph 4.3 two different kinds of actuators are available, patch and stack actuators. For building applications, feasibility and aesthetical considerations suggest that stack actuators are preferred, as their smaller size interferes less with visibility and transparency and allow them to be easily mounted and dismantled from glass surface.

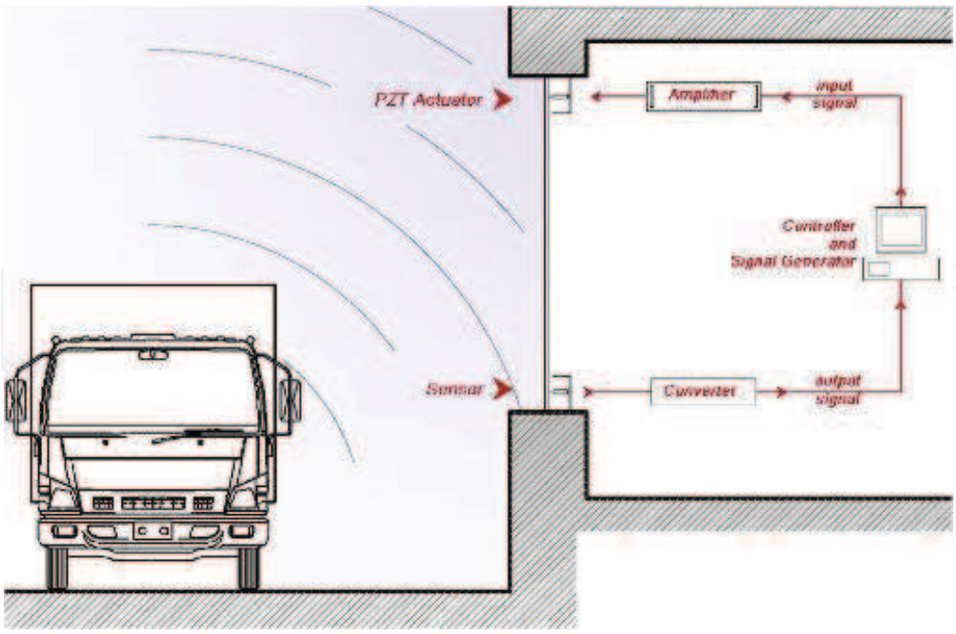

Fig. 10. Layout of the ASAC control system for glazed facades

5.2 The functioning of ASAC System for glazed facades

Signal coming from the sensors is elaborated by charge amplifiers, that convert voltage signals into physical variables like displacements, velocity and accelerations, and by electronic filters, that separate the total vibration field into one due to the primary disturbance from the other connected with the action of secondary sources. The electronic controller, starting from the error signal, estimates the radiated field in some positions of the receiving room and then computes the opportune voltage to be supplied to the actuators in order to reduce the panel's acoustic efficiency. Signal amplifiers provide for necessary electric power.

The optimization of the actuator's actions, in order to minimize the number and the size of the employed sensors and actuators, is derived from opportune algorithms implemented in the controller, like the one presented in (Clark & Fuller, 1992), based on the quadratic linear optimum control theory (see paragraph 4.2). It consists of two parts, the first dedicated to the determination of actuator size and location and the second to sensors. In both parts, the core algorithm computes the voltage to be supplied to the actuators in order to reduce glass vibrations, while the rest of the procedure defines the best actuators' configuration, upon determination of constraints relative to plate's geometry and design choices.

5.3 The technological solution developed as test-case

Stack actuators, as compared to laminated actuators, need a stiffener in order to work properly, hence a technological solution to realize this stiffener has to be designed. The presence of the stiffener, according to its position on the glass surface, may also determine interference problems with the aesthetical appearance of the glass panel which cannot be disregarded. First of all, in order to minimize the radiation efficiency of the vibrating glass surface, the correct positioning of stack actuators has to be studied. Two are the possible ways:

- by decreasing the vibration amplitude of flexural waves (Fig. 11-a);
- By changing the original vibration in order to obtain a vibration field where only even modes dominate (Fig. 11-b).

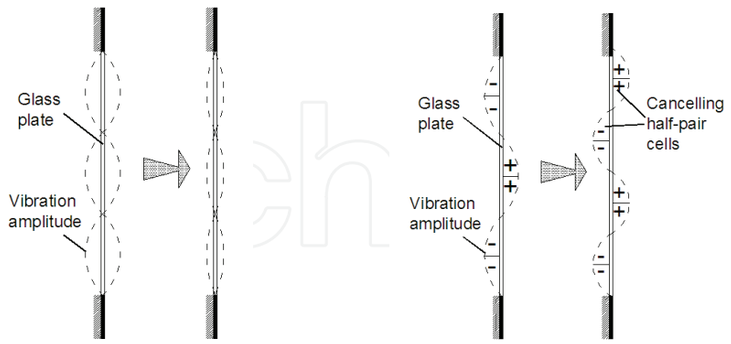

a) b)

Fig. 11. Reduction of the overall acoustic radiation efficiency

In the first case actuators should act in order to reduce vibration amplitudes, while in the second one they should generate a vibration field with less radiation efficiency. To each of the alternatives listed corresponds a different positioning of actuators: in the first case they have to be installed in the points where maximum vibration amplitudes are monitored, while, in the second one, they have to be moved along the border lines, with less interference in glass panel's appearance. Starting from these considerations, in Fig. 12 three possible technological solutions are depicted (Naticchia and Carbonari, 2007):

a. stack actuators positioned close to the central axis, usually characterized by maximum amplitude vibrations, and stiffened by a metal profile (approach 1);
b. stack actuators installed along one border of the panel and stiffened by an angular profile (approach 2);
c. stack actuators placed close to the borders and stiffened with point reaction systems (approach 3).

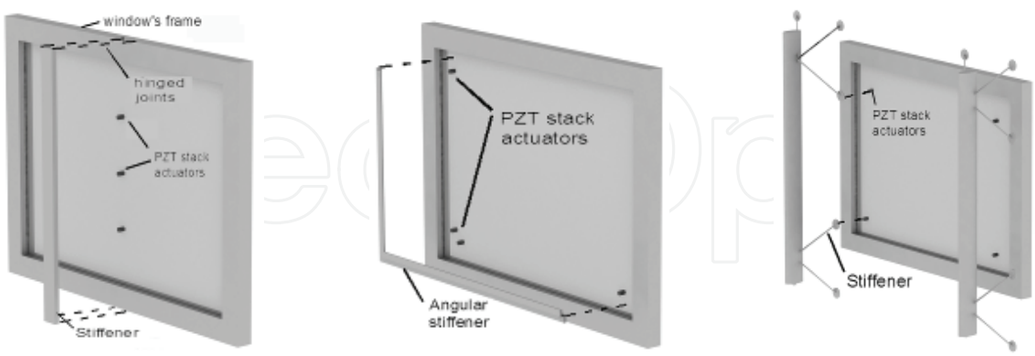

a) b) c)

Fig. 12. Technologic solutions suggested for the installation of actuators.

Further proposals for technological solutions have been advanced, where the actuator is contrasted by a point reaction system directly attached to the glass panel's surface. For this purpose, the use of two different kinds of metallic profiles have been hypothesized: in Fig. 13-a a circular-shaped profile contrasting a stack actuator is depicted in a 3-D view and a

cross-section view, while Fig. 13-b represents a similar solution realized with a z-shaped profile. Both hypotheses seem to be advantageous from an aesthetical point of view, showing little interference with visibility through the glass, and should be studied relative to profile characteristics and to the stress induced in correspondence of the connection point between the same profile and the glass panel.

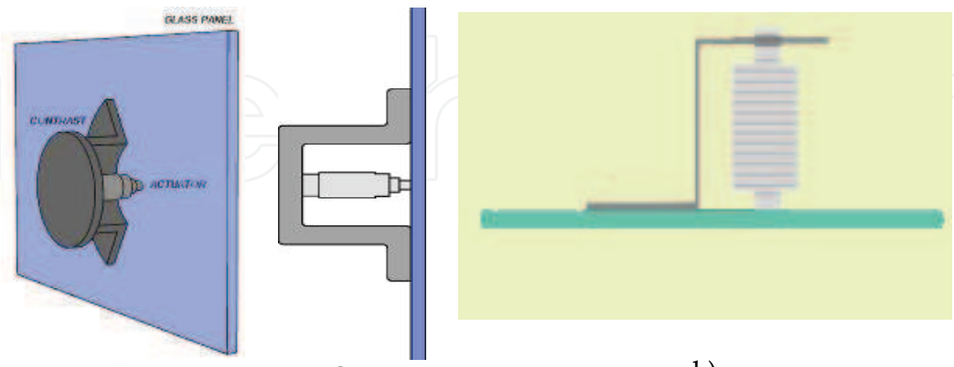

a-1: 3D view a-2: Section b)

Fig. 13. Further hypotheses of point reaction systems: circular-shaped profile (a-1;a-2); Z-shaped profile (b).

For the acoustic simulations carried out and discussed in this chapter, in order to evaluate the effectiveness of the purposed technology over the limits imposed by the choice of one solution with respect to another, an experimental solution has been developed, employing a stack actuator, stiffened by a mass, realized with a cylinder of metallic material overlapped and connected to the free extreme of the actuator, as will be detailed in paragraph 6.2.

6. Experimental analysis

In the following paragraphs, the results of experimental and numerical analyses carried out to evaluate acoustic improvements deriving from the application of the suggested active control technology will be presented (Carbonari and Spadoni, 2007). For this purpose, a finite element model and an experimental prototype were built: in both models the stiffener has been simulated with a 0.177 *Kg* weighted mass contrasting the free extreme of the actuator (Fig. 15-e and 15-f).

6.1 The building of the experimental prototype

Experimental simulations were performed on a prototype, realized by assembling a (1.00x1.40) *m* sized glazed pane with an aluminium profile frame. The main problem regarding the realization of the prototype was the simulation of a simply supporting boundary constraint: it was pursued with the interposition of two cylindrical Teflon bars between the glass panel and the two window frame profiles, as can be seen in Fig. 14-a. Every screw fixing the glass panel in the window frame was subjected to the same torque (through the use of a dynamometric spanner) equal to 0.1 *N·m*, in order to guarantee uniform contact between the glass and the Teflon bars. The whole system, as shown in Figure 14-b, was placed over dumping supports in correspondence of each panel edge, to avoid the influence of external actions on the glass's vibrations, establishing the simplest boundary conditions. A seventy-seven point grid was defined on the panel, in order to identify measurement marks.

6.2 The modal analysis performed on the prototype

The purpose of the experimental analysis is to collect data in order to evaluate the reliability of the finite element model, on which the acoustic simulations will be performed. First of all, a modal analysis was carried out on the prototype in order to determine its natural frequencies. The experimental apparatus employed for the measurements consisted in:

- a transducer for exciting the system (Fig. 15-a);
- an accelerometer for checking the vibration field (Fig. 15-b);
- a PXI platform for collecting data (Fig. 15-c).

National Instruments PXI is a rugged PC-based platform for measurements and automation systems, provided by the Mechanical Measurement Laboratory of the Polytechnic University of Marche (Castellini, Revel, Tommasini, 1998; Castellini, Paone, Tommasini, 1996), whose staff contributed to these experimental tests. PXI is a deployment platform, serving applications like manufacturing test, aerospace and military, machine monitoring, automotive and industrial tests. It is composed of three basic components: chassis, system controller and peripheral modules. PXI can be remotely controlled by PC or laptop computers, but it can also provide for embedded controllers, which eliminates the need for an external controller. In the case of the performed tests, the PXI was connected to a PC monitor in order to display the data collected from measurements on the experimental prototype used to perform its two modal analyses (see Fig. 17-b).

Experimental tests were carried out in the Advanced Robotics Laboratory of the Department of Software, Management and Automation Engineering-DIIGA ("Dipartimento di Ingegneria Informatica, Gestionale e dell'Automazione") of the Polytechnic University of Marche (Antonini, Ippoliti, Longhi, 2006; Armesto, Ippoliti, Longhi, Tornero, 2008), which is equipped with:

- one Wave Generator Hameg Instruments mod. Hm 8030-3 (see paragraph 6.3);
- one Tektronix TDS 220 oscilloscope;
- one National Instruments acquisition card mod. NI USB6009 (see paragraph 6.3).

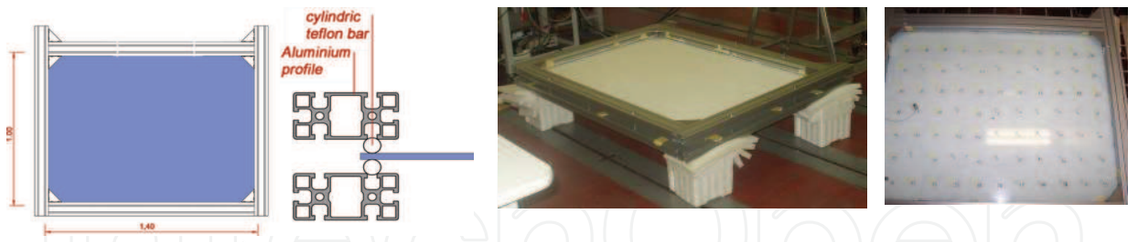

a) b) c)

Fig. 14. The prototype used to realize simply supporting constrains (a), the window frame prototype on the dumping supports (b), Seventy-seven point grid marked on the glazed pane (c).

Modal analysis was first performed on the prototype as depicted in Fig. 14-b, that is on the prototype without any control system component in order to evaluate its natural frequencies. Subsequently, the same tests were repeated on the prototype equipped with the Device Kit, consisting in:

- one actuator acting as control system (in this first stage of the tests, the actuator was inactive to study the system's free vibration);
- one load cell for recording the values of the forces provided by the actuator;

- one stiffening mass for simulating the presence of the stiffener (total weight of the stack actuator device kit was 0.177 *Kg*).

The elements were assembled as shown in Fig. 15-e and 15-f: the stack actuator device kit was positioned along the main axis of the prototype, at a distance of 0.24 m from the edge and fixed to the glass panel with resin. Measurements were carried out keeping the position of the accelerometer unchanged and exciting each one of the seventy-seven grid point with the transducer. The data collected were processed with appropriate software in order to restore the glass panel's modal forms.

From the comparison of the natural frequencies recorded for the two, different, tested systems, summarized in Tab. 4, a maximum percentage error greater than 10% was checked, so that it had been possible to conclude that the presence of the Device Kit, with its volume and its total weight of 0.177 *Kg*, can not be omitted for the development of a correct finite element model.

m,n MODES	1.1	2.1	1.2	3.1	2.2	3.2	4.1	1.3
Prototype + Dev. Kit(Hz)	25.5	47	66.5	85	89	116.5	133.5	141
Not Controlled Prototype (Hz)	25.50	47.50	67.00	85.50	89.00	129.50	134.50	141
ABS. ERROR %	**0.00**	**1.05**	**0.75**	**0.58**	**0.00**	**10.04**	**0.74**	**0.00**

Tab. 4. Comparison between natural frequencies values in the case of non controlled glass panel and of the glass panel with the stack actuator device kit

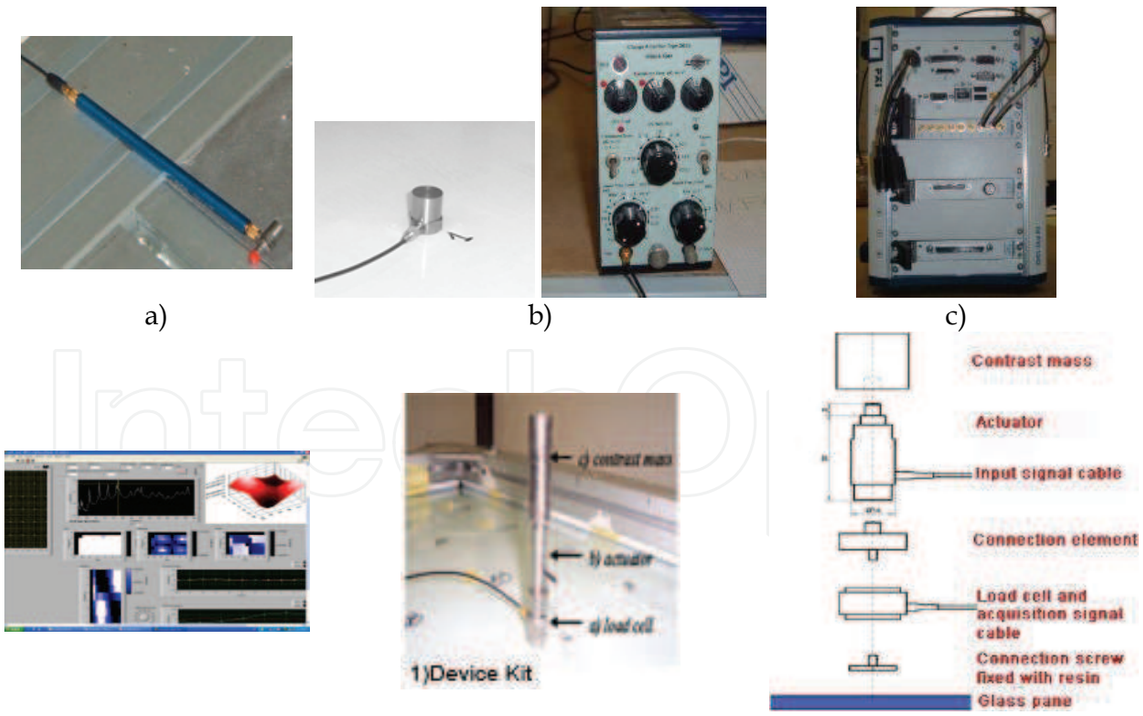

a) b) c)

d) e) f)

Fig. 15. Transducer (a), accelerometer B&K with its amplifier (b), PXI platform (c), modal analysis processing software (d), the stack actuator device kit (e,f).

6.3 The harmonic analysis performed on the prototype

In the second stage of the experimental measurements, harmonic analyses were performed on the prototype, in order to determine the structural response of a window pane, when excited by harmonic force. For this purpose, two frequencies were selected, 81 Hz and 142 Hz, which are very close to the panel's natural frequencies, previously defined for modes (3,1) and (1,3). This choice was influenced by the two following considerations:

- maximum structural response is recorded when a system is excited close to its natural frequencies;
- for the assumed control theory, maximum efficiency is obtained controlling modes with the maximum acoustic efficiency. From previous studies (Naticchia and Carbonari, 2006), it is possible to establish that they are coincident with the glass panel's natural frequencies, with particular reference to (3,1) and (1,3) modes.

For experimental measurements the same apparatus described in paragraph 6.2 was employed, with exception of PXI platform, replaced by the National Instruments Acquisition Card depicted in Fig. 16-a.

a) b) c)

Fig. 16. National Instruments acquisition card mod. NI USB6009 (a), Wave Generator Hameg Instruments mod. Hm 8030-3 (b) and E-610.00 PI amplifier employed for experimental measures (c).

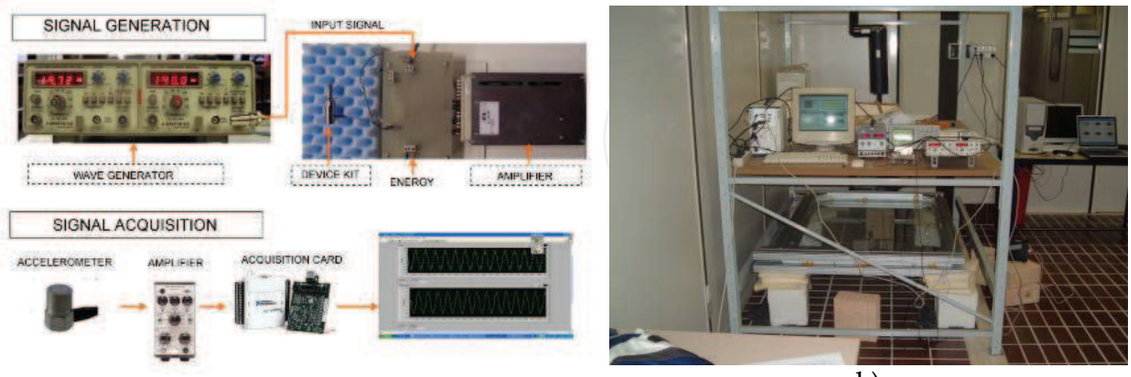

a) b)

Fig. 17. Functioning scheme of the performed tests (a), Experimental apparatus installed in the Advanced Robotics Laboratory of DIIGA of the Polytechnic University of Marche (b).

Differently from the modal analysis, the harmonic analyses were directly performed on the prototype equipped with the Device Kit. The test functioning scheme is represented in Fig.

17-a: harmonic signals exciting the prototype were generated by an analogue Wave Generator (Fig. 16-b) and sent to the Device Kit, passing through the amplifier depicted in Fig. 16-c. The measurements were carried out moving the accelerometer from one point to another of the seventy-seven point grid defined on the glass panel; signals coming from the accelerometer were collected with NI acquisition card and elaborated, with the application of opportune filtering executed using appropriate software. Applying the harmonic motion equation:

$$W_{max} = \frac{a_{max}}{(2\pi f)^2} \tag{19}$$

at every point it was possible to compute displacements along the main axis and along the axis passing through the actuator: displacements diagrams are represented in paragraph 7.3, where they will be used to validate the finite element model.

7. Numeric analysis

7.1 The modal and harmonic analyses performed on the finite element model

The finite element theory was employed for building the numerical model of a window subject to acoustic simulations for the evaluation of the real effectiveness of the technology suggested.

The same characteristics of the experimental prototype, in terms of geometry, material properties and boundary conditions, were reproduced in the finite element model. To this purpose, two different models were implemented in ANSYS 8.0™ environment: the first one represents a rectangular (1.40 x 1.00) *m* large glass plate, simply supported along the whole board (Fig. 18-a). In order to reach a high accuracy level, the plate was subdivided into square shaped finite elements of 0.02 *m* per side. The following parameters for glass material were inputted:

- elasticity Modulus E= 6.9 x 10^{10}Pa;
- Poisson Coefficient ν=0.23;
- density ρ=2457 Kg/m³.

The second model was realized, adding to the first a (0.02x0.02x0.02) *m* sized parallelepiped volume to simulate the Device Kit (Fig. 18-b). In the positioning of the volume on the glass plate the same conditions as the experimental tests were respected and steel-like characteristics were assigned to it:

- elasticity Modulus E= $2.1 \cdot 10^5$ MPa;
- Poisson Coefficient ν=0.33;
- density ρ=22158 Kg/m³ (density value was computed according to the real weight of the Device Kit).

The nomenclature of the glass natural modes was chosen according to the number of troughs along the major and secondary axes of the plate respectively.

Modal analyses were performed on both models and the results were compared, confirming that the presence of the Device Kit cannot be neglected when realizing a proper finite element model: in fact, the comparison of the model forms revealed deviation between the two models, increasing for frequencies higher than 100 Hz. Diagrams and natural frequencies values recorded for the Device Kit equipped model are represented in Fig. 19.

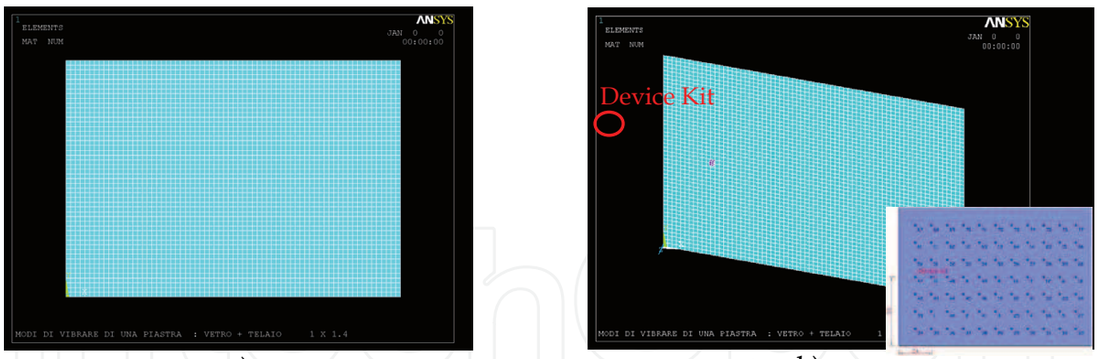

a) b)

Fig. 18. Finite elements model of the glass panel (a), Finite elements model of the glass panel with the Device Kit (b).

According to the results of the modal analysis, harmonic analysis was performed exclusively on the Device Kit equipped pane model. To this aim a point force was applied on the Device Kit volume, with an intensity of 0.17 *N* (the same value recorded by the load cell during experimental tests) at the two different frequencies of 81 Hz and 142 Hz. Results will be discussed in the following paragraph.

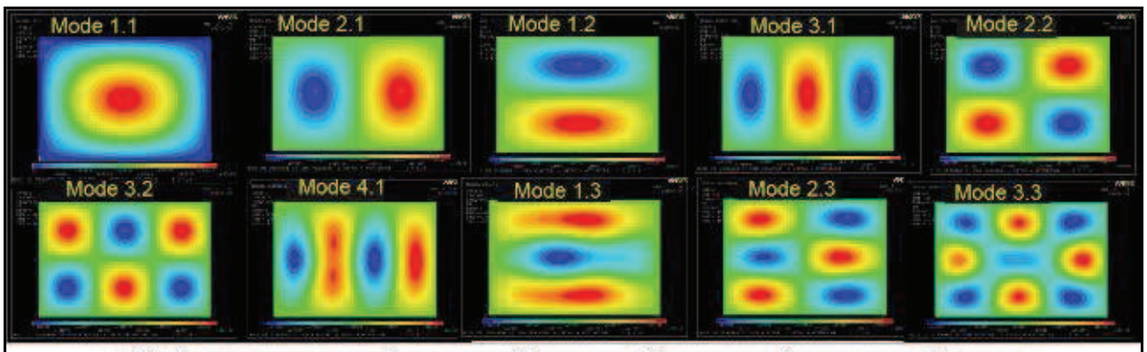

Modes m,n	1	2	3	4	5
1	22.291	66.913	140.72	245.25	379.4
2	44.498	89.503	161.75	267.52	401.57
3	81.515	127.18	197.72	304.69	438.55
4	133.94	180.08	250.92	357.16	490.38
5	203.7	248.23	319.96	424.45	557.12

Fig. 19. Modal shapes and the corresponding natural frequencies of the Device Kit equipped model.

7.3 The validation of the finite element model

Reliability of the finite element model was demonstrated through the comparison between the experimental and the numerical results. First of all, the results of the modal analysis were compared, revealing a good agreement between the values of natural frequencies for the experimental and the finite elements model: actually, a maximum percentage error of 3% was recorded.

Subsequently, diagrams relative to displacements recorded for the numerical and experimental model, due to the harmonic analysis at 81 and 142 Hz were superimposed, as represented in Fig. 20.
It can be noticed that there is a good superposition between the two models: in fact a maximum percentage difference of about 4,5% at 81 Hz frequency and of about 15% at 141 Hz frequency were registered, with an average difference of about 10%. According to these acceptable deviations, also ascribable to local effects not contemplated by the numerical model, it was considered reliable and was used for performing the acoustic simulations.

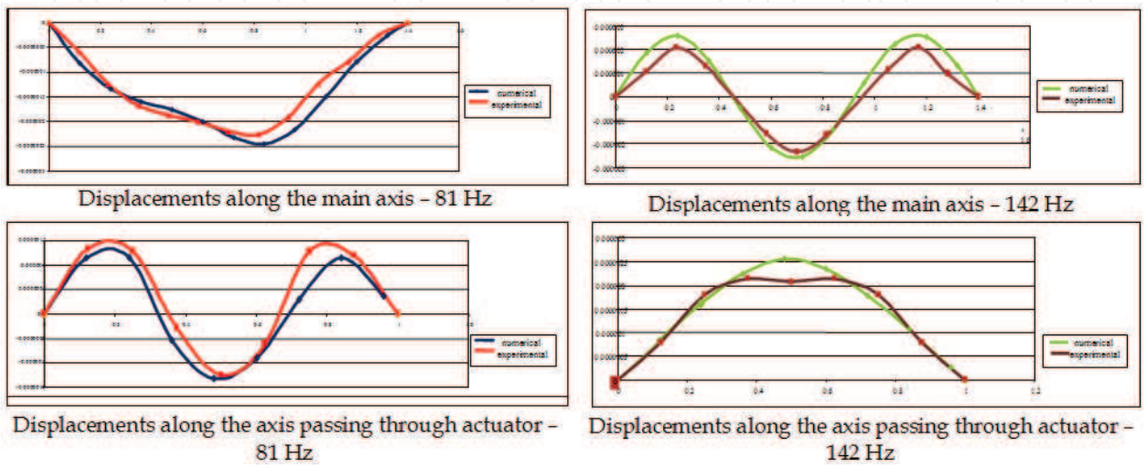

Fig. 20. Comparison between displacements diagrams for experimental and numerical harmonic analysis.

7.4 The evaluation of sound transmission loss improvements due to the ASAC system

For an acoustic evaluation of the suggested technology, the finite element model, developed in ANSYS 8.0™ environment, was imported in LMS VIRTUAL LAB™ environment which is another finite element software, containing two dedicated sections named *noise and vibration* and *acoustics* (the first section was used to perform modal analysis and the second for the acoustic evaluations). Simulations were carried out in order to have numerical results concerning the real effectiveness of the suggested ASAC control system.
It is well-known that one of the most recurring and irritating noise sources is represented by urban traffic, especially connected with heavy vehicles, such as lorries. A research have demonstrated that a lorry, travelling a low distance and at a speed of 70 Km/h produces a noise level equal to 85 dB (Fig. 2), within a range of frequencies in which the dominant one can be identified at 140 Hz, corresponding to the glass panel's natural vibration mode (1,3). According to these assumptions, a test room measuring (2.40x2.50x2.80) *m* was developed for simulations, including within one of the walls, the validated glass panel (please refer to Fig. 21-a).
In previous research activities simulations have been led to evaluate achievable noise level reduction by the application of the ASAC technique, without considering the influence ascribable to the presence of a stiffener or a stiffening mass for the correct functioning of the

actuator. In the above case, a reduction of about 15 dB in the disturbance pressure noise was estimated (Naticchia & Carbonari, 2006). Results of simulations presented in this paragraph instead, can be considered more realistic, as it also takes into account the presence of the stiffener. The developed test room was analyzed in two different configurations:

1. *anechoic room*: every wall of the room was made up of totally absorbent panels;
2. *reverberant room*: acoustic properties were associated to every wall of a typical building material like plaster for the ceiling, wallpaper for vertical walls and carpet for the floor.

In both cases, the disturbing wave incident on the glazed panel was assimilated to a uniform constant pressure on the panel equal to 0,3556 Pa, applied at the frequency of 140 Hz: this condition seems to be realistic, considering the distance that usually separates the windows of a building from the street, source of the noise. The acoustic pressure level within the room was evaluated for the following conditions:

1. acting disturbance;
2. acting actuator;
3. simultaneous acting of disturbance and actuator.

The results of the simulations are represented in Fig. 21-b with coloured diagrams relative to the anechoic room and to the reverberant room, with reference to the acoustic pressure recorded on the walls of the room with and without the application of the proposed ASAC system: the numerical values of the recorded pressure levels for both cases are synthesized in Tab. 5.

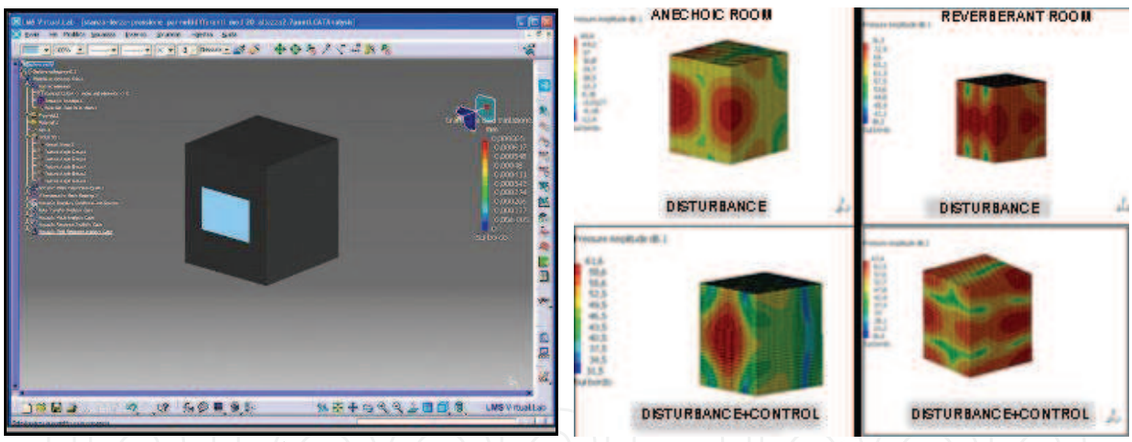

a) b)

Fig. 21. The test room model used for the acoustic simulations in LMS™ environment (a), diagrams of the noise level recorded in the anechoic room (left side) and in a real room (right side) with and without the application of ASAC system(b).

According to these results, the first observation that can be derived is that, even if the reduction achievable in the disturbance pressure level is greater in the case of the anechoic room than it is in the reverberant room, as would be expected, nevertheless in the real case, there is a sensitive drop of about 10 dB in the noise level transmitted within the room.
Besides this, it can be stated that the presence of the stiffener cannot be omitted for a real acoustic evaluation of the technology suggested.

Average interior noise level recorded with the acoustic simulations (dB)		
	Reverberant Room	Anechoic Room
Disturbance (0,3556 Pa;140Hz)	76,7	61,6
Disturbance + Acting Actuator	67,4	49,4
Maximum recorded decrease	9,3	12,2

Tab. 5. Final results of the acoustic simulations performed in LMS Virtual Lab ™ environment

8. Conclusions

In these pages it was demonstrated that the Active Structural Acoustic Control can be successfully applied in the building field, in order to provide a major improvement in glass panels' sound transmission loss in the low frequencies range: the employment of just one actuator causes a sensitive drop in the noise transmitted from the exterior to the interior, allowing the achievement of the restrictive requirements imposed by European and Italian standards. At the same time, initial considerations were presented in order to investigate the feasibility of a technological solution based on the active control of vibrations.
In order to prepare this technology for use in buildings, further efforts should be directed to facing the following two different aspects:

1. experiments using more than one actuator, to control some of the most efficient modes should be carried out, in order to determine the effects due to the interaction of different actuators and then to evaluate the final noise drop transmitted from the exterior to the interior;
2. simulations and laboratory experiments should be directed to develop a technological solution allowing the proper integration of the Active Structural Acoustic Control system with a glazed panel's structural frame.

In addition, the same technique could be adopted for applications on other specialized products such as light opaque building partition walls, railway and traffic noise shielding, temporary environmental noise barriers or even real-time controlled reflecting panels for the acoustic adjustment of concert halls

9. References

Antonini, P., Ippoliti, G., Longhi, S., (2006), Learning control of mobile robots using a multiprocessor system, *Control Engineering Practice*, vol. 14, pp. 1279-1295, ISSN: 0967-0661.

Armesto, L., Ippoliti , G., Longhi, S., Tornero, J., (In press June 2008), An asynchronous multi-rate approach to probabilistic self-localisation and mapping. *Ieee Robotics And Automation Magazine*. ISSN: 1070-9932.

Bao, C. and Pan, J., (1997), Experimental study of different approaches for active control of sound transmission through double walls, *Journal of the Acoustical Society of America*, vol. 102(3), pp. 1664-1670.

Baumann, W. T., Ho, F. S., Robertshaw, H. H., (1992), Active structural acoustic control of broadband disturbances, *Journal of the Acoustic Society of America*, 92(4).

Baumann, W. T., Saunders, W. R., Robertshaw, H. H., (1991), Active suppression of acoustic radiation from impulsively excited structures, *Journal of the Acoustic Society of America*, 90(6).

Burdisso, R.A. and Fuller, C.R., (1994), Design of active structural acoustic control systems by eigenproperty assignment, *Journal of the Acoustical Society of America*, Vol. 96, No. 3, pp. 1582-1591.

Carbonari, A. and Spadoni, S., (2007), An Active technology to increase sound transmission loss of glazed facades, *Proceedings of ARTEC Conference "The Building Envelope – a complex design"*, pp. 199-206, ISBN 978-88-6055-223-5, Ancona, November 2007, Alinea, Firenze

Castellini, P., Paone, N., Tomasini, E. P., (1996), The Laser Doppler Vibrometer as an Instrument for Non-intrusive Diagnostic of Works of Art: Application to Fresco Paintings, *Optics and Lasers in Engineering*, Vol. 25, pp. 227-246, Elsevier Science Ltd., Northern-Ireland.

Castellini, P., Revel, G. M., Tomasini, E.P., (1998), Laser Doppler Vibrometry: a Review of Advances and Applications, *The Shock and Vibration Digest*, vol. 30(6), pp. 443-456, Sage Science Press, Thousand-Oaks, CA

Chaplin, G.B.B. and Smith, R.A., (1976), Active Methods of Cancelling Repetitive Vibrations, *U.K. Patent 1,971,7176*.

Clark, R.L. and Fuller, C.R., (1992), Optimal placement of piezoelectric actuators and polyvinylidene fluoride error sensors in active structural acoustic control approaches, *Journal of the Acoustical Society of America*, Vol. 92, No. 3, pp. 1521-1533.

Clark, R.L., Fuller, C.R., Wicks, A., (1991), Characterization of multiple piezoelectric actuators for structural excitation, *Journal of the Acoustical Society of America*, Vol. 90, No. 1, pp. 346-357.

Conover, W.B., (1955), Recent contributions to transformer audible noise control, *AIEE Transactions, Applications and Industry*, Vol. 74, Part D, pp. 77-86.

Cunnefare, K. A., (1991), The minimum multimodal radiation efficiency of baffled finite beams, *Journal of the Acoustic Society of America*, 90(5).

Dimitriadis, E.K., Fuller, C. R., Rogers, C.A., (1991), Piezoelectric actuators for distributed vibration excitation of thin plates, *American Society of Mechanical Engineers Journal of Vibration and Acoustics*, 113, pp. 100-107.

Fahy, F., (1985), *Sound and structural vibration – radiation, transmission and response,* Academic Press, London - New York – Boston – Sydney – Tokyo – Toronto, par. 4.3.

Fuller, C. R., Elliott, S. J., Nelson, P. A., (1997), *Active Control of Vibration,* 2nd Edition, Academic Press, San Diego-London- Boston-New York, par. 2.10 – 8.4 – 8.5.

Hall, D. E., (1987), *Basic Acoustics*, John Wiley and sons, New York – Chichester – Brisbane – Toronto – Singapore, pp. 122-124.

Harris, C.M., (1984), *Handbook of Acoustical Measurements and Noise Control*, 3rd edition, McGraw Hill, New York.

Harris, C.M., (1994) *Noise Control in buildings,* McGraw Hill ed., New York.

IMAGINE, (2003), EC Project funded Technical Report WP 1.1: "Source modeling of road vehicles" , IMAGINE - *Improved Methods for Assessment of the Generic Impact of Noise in the Environment.*

Kido, K., (1975), Reduction of Noise by use of Additional Sound Sources, *Proceedings of Inter-Noise 75*, Sendai, Japan, pp. 647-650.

Kaiser, O. E., Pietrzko, S. J., Morari, M., (2003), Feedback control of sound transmission through a double glazed window, *Journal of Sound and Vibration*, vol. 263, pp. 775-795.

Lueg, P., (1936), Process of silencing sound oscillations, *US Patent No. 2,043,416*.

Meirovitch, L., Baruh, H. Öz, H., (1983), A comparison of control techniques for large flexible systems, *Journal of Guidance, Control, and Dynamics*, 6(4), 302-310.

Naticchia, B. and Carbonari, A., (2007): Feasibility analysis of an active technology to improve acoustic comfort in buildings, *Building and Environment*, Vol. 42, Issue 7,pp 2785-2796.

Naticchia, B. and Carbonari, A., (2006), First numerical and experimental results on active controlled glazed facades, *Proceedings of the 23rd ISARC Conference*, ISBN:4-9902717-1-8, Tokyo, October 2006

Nelson, P. A. and Elliott, S. J., (1995), *Active Control of Sound*, Academic Press Limited, London. 3rd printing.

Olson, H.L., and May, E.G., (1953), Electronic sound absorber, *Journal of the Acoustical Society of America*, Vol. 25, No. 6, pp. 1130-1136.

Pan, J., Snyder, S. D., Hansen, C. H., Fuller, C., R., (1992), Active control of far-field sound radiated by a rectangular panel – A general analysis, *Journal of the Acoustic Society of America*, 91(4).

Roussos L. A., (1985), *Noise transmission loss of a rectangular plate in an infinite baffle*, NASA, TR 2398, Washington, DC.

Ruckman, C. E. and Fuller, C. R. (1995), Optimizing actuator locations in active noise control systems using subset selection, *Journal of Sound and Vibration*, 186(3), 395 - 406.

Spagnolo, R. (2001), *Manuale di acustica*, UTET Libreria editions.

Timoshenko, S, Woinolowsky-Krieger, *Theory Of Plates And Shells*, Mcgraw-Hill, 1959

Wang, B., Burdisso, R.A., and Fuller, C.R., (1994), Optimal placement of piezoelectric actuators for active structural acoustic control, *Journal of Intelligent Material Systems and Structures*, Vol. 5, Jan., pp. 67-77.

Yang, D., and Fuller, C.R., (1995), Numerical simulation of active control of interior noise in a business jet with point force actuators - optimization of transducers, *Proceedings of Inter-noise 95*.

Zhu, H., Rajamani, R., Stelson, K. A., (2004), Active control of glass panels for reduction of sound transmission through windows, *Mechatronics*, vol. 14, pp. 805-819.

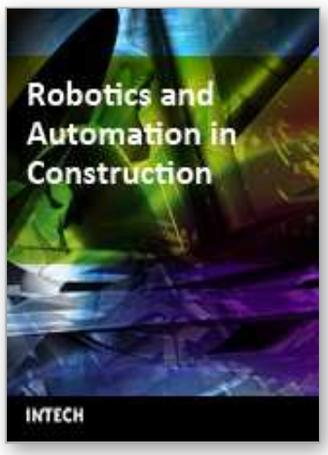

Robotics and Automation in Construction

Edited by Carlos Balaguer and Mohamed Abderrahim

ISBN 978-953-7619-13-8
Hard cover, 404 pages
Publisher InTech
Published online 01, October, 2008
Published in print edition October, 2008

This book addresses several issues related to the introduction of automaton and robotics in the construction industry in a collection of 23 chapters. The chapters are grouped in 3 main sections according to the theme or the type of technology they treat. Section I is dedicated to describe and analyse the main research challenges of Robotics and Automation in Construction (RAC). The second section consists of 12 chapters and is dedicated to the technologies and new developments employed to automate processes in the construction industry. Among these we have examples of ICT technologies used for purposes such as construction visualisation systems, added value management systems, construction materials and elements tracking using multiple IDs devices. This section also deals with Sensorial Systems and software used in the construction to improve the performances of machines such as cranes, and in improving Human-Machine Interfaces (MMI). Authors adopted Mixed and Augmented Reality in the MMI to ease the construction operations. Section III is dedicated to describe case studies of RAC and comprises 8 chapters. Among the eight chapters the section presents a robotic excavator and a semi-automated façade cleaning system. The section also presents work dedicated to enhancing the force of the workers in construction through the use of Robotic-powered exoskeletons and body joint-adapted assistive units, which allow the handling of greater loads.

INTECH
open science | open minds

InTech Europe
University Campus STeP Ri
Slavka Krautzeka 83/A
51000 Rijeka, Croatia
Phone: +385 (51) 770 447
Fax: +385 (51) 686 166

InTech China
Unit 405, Office Block, Hotel Equatorial Shanghai
No.65, Yan An Road (West), Shanghai, 200040, China
中国上海市延安西路65号上海国际贵都大饭店办公楼405单元
Phone: +86-21-62489820
Fax: +86-21-62489821

www.intechopen.com

IntechOpen

IntechOpen